Chapter 10

Probing the Action of Cytochrome *c* Oxidase

Vangelis Daskalakis and Constantinos Varotsis*
Department of Environmental Science and Technology, Cyprus University of Technology, P.O. Box 50329, 3603 Lemesos, Cyprus

Summary

Density functional theory (DFT) and combined Molecular Mechanics/Quantum Mechanics (MM/QM-MD) calculations have been applied to models of the cytochrome *c* oxidase (CcO) including the Fe–Cu_B binuclear center, where dioxygen is bound and subsequently reduced to water. The properties of several intermediates of the CcO dioxygen reaction have been investigated by theoretical approaches. In this chapter, we investigate the dynamics of the binuclear heme Fe–Cu_B throughout the O_2 catalytic cycle. We are focused on the effects of the protein matrix and proton/water motion exerted on the heme a_3 group. For this, we have built models of CcO, which vary at the heme a_3 environment. This variability is based on hydrogen bonding interactions and amino acid protonation states. Different control points have been identified for the transition from one intermediate to the next. The hydrogen bonding networks in the proximity of heme a_3 area also have consequences for the characteristics of the binuclear center. A theoretical framework for the direct link between an H^+ delivery channel (termed D) and an accumulation of waters, termed '*water pool*' close to the active site, has been achieved at the QM/MM level of theory. Two proton valves (E278 and His403) and an electron/proton coupling site (propionate-A/Asp399) exist in this pathway for the aa_3 CcO from *P. denitrificans*. The ferryl intermediate, produced subsequent to the O–O bond scission, is found to have characteristics highly dependent on the basicity of the proximal His411, in contrast to the hydroxyl intermediate that is sensitive to distal effects.

*Author for correspondence, e-mail: c.varotsis@cut.ac.cy

M.F. Hohmann-Marriott (ed.), The Structural Basis of Biological Energy Generation, Advances in Photosynthesis and Respiration 39, pp. 187–198, DOI 10.1007/978-94-017-8742-0_10,

I. Introduction

Theoretical studies are routinely used to probe complex biological systems in atomistic details. These studies include, among others, Density Functional Theory (DFT), Molecular Mechanics (MM) and Molecular Dynamics (MD), as well as combined Molecular Mechanics/Quantum Mechanics (QM/MM) methodologies. Cytochrome *c* oxidase (CcO), a terminal respiratory enzyme (see also Chap. 9), catalyzes the transfer of electrons from the reduced cytochrome *c* to the molecular oxygen and translocates protons vectorially across the mitochondrial inner membrane. Four redox active metal centers are present in the enzyme: two hemes *a* and three associated copper atoms. In eukaryotes, the electrons coming from the substrate cytochrome *c* enter the homodinuclear copper center, Cu_A. From there, electrons are transferred, via the low-spin heme *a*, to the bi-nuclear center containing a high-spin heme a_3 and a Cu_B complex. The latter two metal sites constitute the active catalytic site, where oxygen is reduced to water by four electrons and four protons (Wikström 1989; Babcock and Wikström 1992; Ferguson-Miller and Babcock 1996; Gennis 1998; Michel 1998a, b). The function and proposed mechanisms of action of CcO enzymes have been reported before (Babcock and Wikström 1992; Ferguson-Miller and Babcock 1996; Michel et al. 1998; Belevich and Verkhovsky 2008). Binding of O_2 to the heme a_3-iron leads to the first oxy intermediate $Fe(II/III)_{a3}$–O_2|$Cu_B(I)$, which subsequently is converted to the peroxy $Fe(III)_{a3}$–O—O–|$Cu_B(II)$ species. Reduction by the third and fourth electrons yields the ferryl $Fe(IV)_{a3}$=O|$Cu_B(II)$–OH and hydroxyl $Fe(III)_{a3}$–OH|$Cu_B(II)$–OH intermediates, respectively (Wikström 1989; Babcock and Wikström 1992; Ferguson-Miller and Babcock 1996; Gennis 1998; Michel 1998a, b).

The ferryl intermediate has gained a lot of attention by several research groups (see literature from Babcock, Gennis, Ferguson-Miller, Michel, Varotsis, and Wikström groups), as it presents a key structure produced immediately after the O–O bond cleavage, a step not yet characterized mechanistically in atomistic detail. There was an initial assignment based on the Optical Absorption spectra of the species with a major peak at 580 nm to an oxyferryl (F) heme iron, while the 607 nm species to a ferric heme peroxide (P) structure, and they were named F and P, respectively (Wikström 1981). Later studies attributed an oxo-ferryl character to both species (Varotsis and Babcock 1990; Ogura et al. 1996; Han et al. 2000). The 804/790 cm^{-1} ν(Fe–O) modes in the resonance Raman spectra have been theoretically attributed to the same oxidation level with oxo-ferryl character (P_M) in the CcO dioxygen reaction (Daskalakis et al. 2008). The protonation state of the propionate-A/Asp399 (prop-A/D399) pair seems not to influence significantly the location of the 804/790 cm^{-1} bands but only their intensities. Thus, different protonated/deprotonated states of this pair vary the intensity of one band over the other and their contribution to the experimental spectra. This results in the appearance of one or two prominent positive bands in the difference spectra of isotopically-substituted species such as the ferryl-oxo intermediates in the CcO dioxygen reaction (Daskalakis et al. 2008). Moreover, for the enhancement of the δ(His–Fe=O) ferryl bending mode, we have identified crucial resonances, and linked them to conformational/structural changes during enzymatic turnover, including the Fe–Cu_B distance, which is controlled by

Abbreviations: BLYP – Functional to describe the exchange and correlation part of the electron-electron interaction energy in the theoretical calculations based on Becke's correlation functional; Lee, Yang, Parr exchange terms; CcO – Cytochrome *c* oxidase; DFT – Density functional theory; MD – Molecular dynamics; MM – Molecular mechanics; OPLS – Optimized potentials for liquid simulations force field; QM – Quantum mechanics; riBLYP – Resolution of identity (ri) methodology is an approximation to the computation of two-electron four-center integrals with significantly improved time efficiency; TZVP – Triple-zeta basis sets, TZVP contains a set of d-functions on the heavy atoms and one set of p-functions on hydrogen atoms

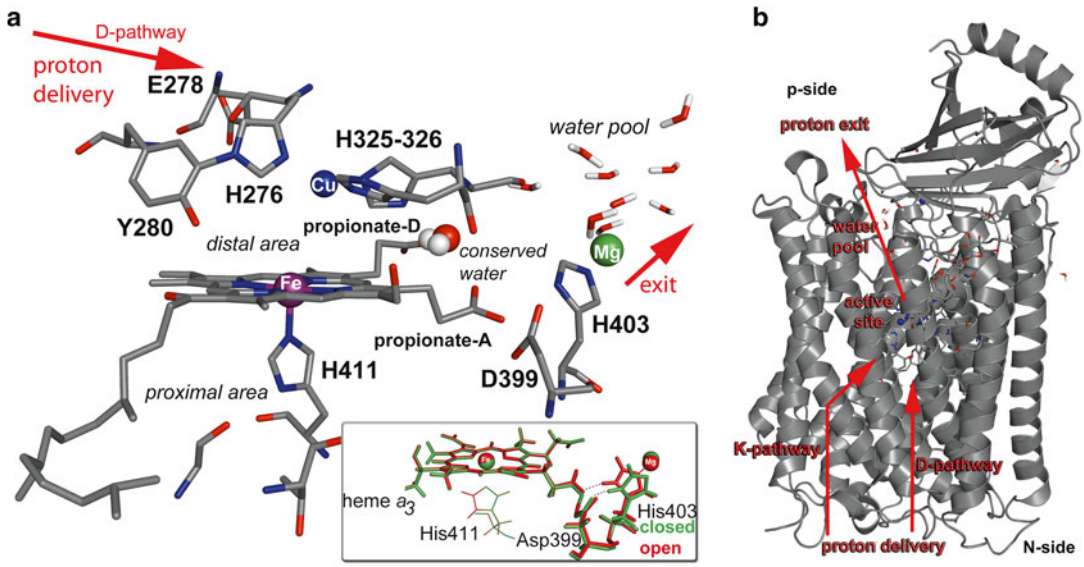

Fig. 10.1. Cytochrome *c* oxidase from *P. denitrificans*. (**a**) Active site with His403 conformations are shown in the inset. Most important surrounding amino acids are also visible. Glu278 is depicted as part of the proton delivery channel termed D-pathway. (**b**) Proton delivery channels (K- and D-pathways), as well as some waters in the water pool can be seen in the structure.

electrostatic interactions in the active site and especially in the area of the heme a_3 propionates (Daskalakis et al. 2011). The position of Cu_B in respect to the heme a_3 plane appears also sensitive to the protonation events in the propionates. In addition, we have proposed that conformational changes in the region of the ring A propionate of heme a_3, due to protonation events, are communicated via the Asp399/His403 pair to Gly386/Thr389 in the proximal area, thereby altering the Hydrogen bonding networks in the region. This, in turn, controls the effect of proximal ligand His411 to the frequency of the ferryl Fe=O bond.

In order to identify the key effects of the protein matrix on the CcO active site, we start by studying several crystal structures of the aa_3–CcO solved to date (Iwata et al. 1995; Tsukihara et al. 1995; Ostermeier et al. 1997; Yoshikawa et al. 1998; Koepke et al. 2009). The fifth axial ligand of heme a_3–Fe is a histidine, termed His proximal. In this proximal area, Gly and Thr residues are also found in the crystal structures of aa_3 from *Paracoccus denitrificans* (Ostermeier et al. 1997) and bovine heart (Koepke et al. 2009), while the ba_3 from *Thermus thermophilus* lacks the Thr residue; instead, a second Gly is located at the proximal site (Soulimane et al. 2000; Hunsicker-Wang et al. 2005). Oxygen binds as the sixth axial ligand, distal to heme a_3 area, between heme a_3 and the Cu_B metal. The latter is coordinated to three His residues. One of the unique properties of the binuclear center, determined by the crystal structures and conserved among different CcOs (Rauhamäki et al. 2006), is the covalent link between a Tyr residue and one of the three His ligands of Cu_B. The cross-linked Tyr forms an hydrogen bonding interaction with the hydroxyethyl-farnesyl side chain of heme a_3. This cross-linked Tyr is also in hydrogen bonding distance to the substrate oxygen in the distal area. Figure 10.1a shows the heme a_3–Fe site of CcO from *P. denitrificans* (Koepke et al. 2009) indicating the *proximal* and *distal* regions, as well as the most important amino acids in the vicinity of the active site.

It has been previously reported that hydrogen bonding networks affect the basicity of the axial to the heme iron ligand to support oxidation states of heme iron greater than III

(Goodin and McRee 1993; Vogel et al. 1999). Cytochrome *c* oxidase, sulfite reductase and the carbon monoxide-sensing heme protein (CooA) exhibit such proposed hydrogen bonding networks (Goodin and McRee 1993; Crane et al. 1997; Vogel et al. 1999). In the case of CcO, a proton movement through hydrogen bonding networks also induces changes in the vibrational spectroscopic characteristics (Daskalakis et al. 2008, 2010). Moreover, hydrogen bonding to the Nδ–H hydrogen (Fig. 10.1a) of the proximal His is the crucial step in understanding how reactivity of the heme-iron is controlled proximally in proteins (Decatur et al. 1999). On the other hand, protonation of the substrate oxygen, which is achieved most likely through hydrogen bonding interactions at the distal site, is crucial for the H_2O production in the CcO/O_2 reaction. Thus, it is of great importance to probe the sites proximal and distal to heme a_3 that are influential during the reduction of O_2 by CcO. Hydrogen bonding networks can be altered by proton and water motion throughout the catalytic cycle of the CcO enzyme. The transfer of a proton (H^+) from E278 (*P. denitrificans* numbering) to an unknown residue above hemes a/a_3 is the first step mediated by CcO that leads to the translocation of protons across the mitochondrial membrane. During the P → F transition, E278 is protonated via the D-pathway. This proton is subsequently transferred to the active site and E278 is re-protonated, while another proton is released to the P-side, as indicated in Fig. 10.1b (Bellevich et al. 2006), as it can be seen in Fig. 10.1b. Several approaches have been used to predict either long distance (QM/MM, MD) or short distance (DFT) effects in models of CcO from proton and electron transfer processes.

II. The Dioxygen Activation Models

Theoretical studies of electron and proton transfer events in the CcO enzyme are a crucial tool for elucidating the interactions between metals, prosthetic groups, ligands and the protein matrix. In addition to insights specifically relevant for the CcO enzymes, these studies also elucidate important aspects into the action mechanisms of other heme proteins involving proximal and distal to heme interactions.

Hydrogen bonding networks, like electron transfer pathways, play a significant role in the double function of heme-copper oxidases: (a) to reduce molecular oxygen to water and (b) to pump protons across the inner mitochondrial membrane. DFT, MD, QM/MM calculations on heme-copper center models provide profound insight into the structural, electronic and dynamic properties of several intermediates throughout the catalytic cycle of O_2 reduction in cell respiration (Blomberg et al. 2000a, b, 2003; Bassan et al. 2006; Kozlowski et al. 2006).

In this chapter we elucidate the heme proximal and distal dynamics and quantify the effects of hydrogen bonds in the regions around the active site for several intermediates in the dioxygen activation catalytic cycle. Experimental quantification would be difficult, as only overall differences in the hydrogen bonding networks could be measured. Furthermore, atomistic details of such reaction dynamics are accurately probed by theoretical calculations.

The crystal structure of aa_3 cytochrome *c* oxidase from *P. denitrificans* (PDB 1AR1) provides the initial x, y, z Cartesian coordinates for the atoms of each model studied. The size of the model depends on the theoretical methodology used. In DFT calculations we restrict our systems to the active site including the first coordination sphere for each metal (Fe_{a3}–Cu_B) and some of the hydrogen bonding networks in the proximal region, while QM/MM-MD calculations encompass the whole protein in a water solvent.

DFT calculations were performed to probe the proximal and distal effects on the CcO heme a_3 active site. For the DFT, ethylic acids can be used in the proximal region, near heme-iron axial ligand, to reproduce the hydrogen bonding network found in the area, thereby substituting the Gly and/or Thr residues. Carbonyl groups of the peptidic bonds

in the enzyme, found near the proximal His, are in this way represented by carboxyl groups donating the electronegative atom in the hydrogen bonding network. Ethylic acids are found to be quite convenient small molecules for the study that do not introduce unwanted hydrogen bonds or other interactions in the proximal region. For each structure considered, a full geometry optimization was performed on riBLYP/TZVP level of theory using the *Turbomole V.5-8-0* software package (Turbomole 2005). For metals (iron and copper) an effective core potential (ECP) is applied (termed "ecp-10-mdf" for iron and "ecp-18 arep" for copper atom), as implemented in *Turbomole software package*. Moreover, we have implemented the computational advantage of the RI-J (*Resolution of the Identity*) approximation (Billingsley and Bloor 1971; Eichkorn et al. 1995), as defined in *Turbomole* with the default parameterization. Geometry optimized DFT models of the active site of CcO with relevant vibrational frequencies are presented in Fig. 10.2.

A mixed quantum mechanics/molecular mechanics (QM/MM) approach was used to probe protonation/deprotonation and water motion events near the active site of CcO. QM/MM calculations can seamlessly join together QM and MM representations of a complex system. The fundamental idea is to divide a large, condensed phase system into two regions; the reactive chemical event is contained within the QM region (which includes the active site as in the DFT calculations), while the surrounding condensed phase is modeled via molecular mechanics. The DFT/MM calculations were performed using the QSite module of Schrodinger 2010 Suite of Programs (Schrodinger). B3LYP functional and lacvp* basis set was used for the QM part, while the OPLS2005 force field (FF) was used for the MM part throughout this work.

We prepared initial structures for the QM/MM calculations, by varying the protonation state of propionate-A and Asp399 carboxylic groups. We have built complete models of the solvated CcO protein by adding missing hydrogen atoms and a water buffer of more than 14 Å (T3P FF) between the protein matrix and the boundaries of the simulation box. Crystallographic waters, inside the protein structure, were retained before and after the solvation. An initial minimization/relaxation process was performed by the Desmond Software of Schrodinger Suite 2010, before each QM/MM calculation. The relaxation was based on the default protocol proposed in the Desmond manual. This included stages of solute-restrained minimization, no restrain minimization, NVT simulation of 24 ps, 10 K, NPT simulation of 10 K, 1 atm, NPT simulation of 24 ps, 300 K and 1 atm with non-hydrogen solute atoms restrained and a final NPT 24 ps simulation at 300 K and 1 atm (Schrodinger). For the QM/MM geometries after the minimization/relaxation, we reduced the water buffer significantly by excluding every solvent molecule beyond a distance of 8 Å away from the protein matrix and restrained to their coordinates those waters beyond a 20 Å layer around the heme iron according to their minimized positions. A cutoff distance of 100 Å was also set for the Coulombic interactions. The hydrogen-cap approach was used for the covalent QM-MM boundary region, where hydrogen atoms are used to "cap" the QM-cut/unsaturated bonds. Gaussian charges were implemented to provide the electrostatic contribution from the MM part to the QM Hamiltonian. Figure 10.3 depicts a typical QM/MM system under study.

III. Proton and Water Motion Drives the CcO Dioxygen Reaction

A. The Oxy Intermediate

In the oxy intermediate, DFT calculations show that the O–O bond strength is not at all affected by the proximal hydrogen bonding network (Fig. 10.2, models 5–6/5w). The O–O weakening in this phase of the catalytic cycle is not favored by either the proximal, nor by the distal interactions. So how does the enzyme proceed to the next intermediate?

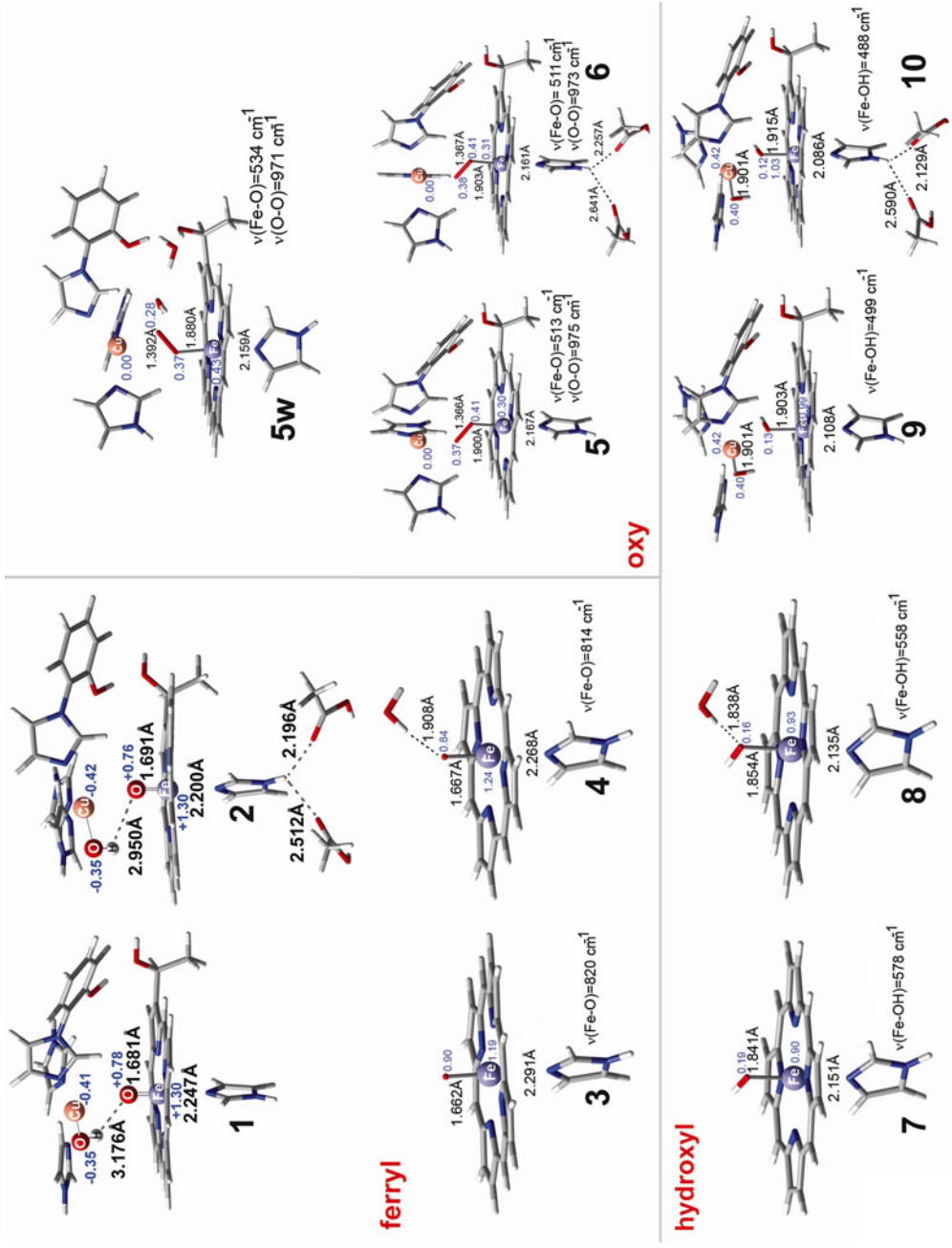

Fig. 10.2. Geometry optimized structures of DFT models of the active site of CcO in different oxidation levels. Selected interatomic distances (imidazole–Fe, Fe–O and O–O) are also shown, as well as selected spin populations in *blue* (Fe, Cu, and O).

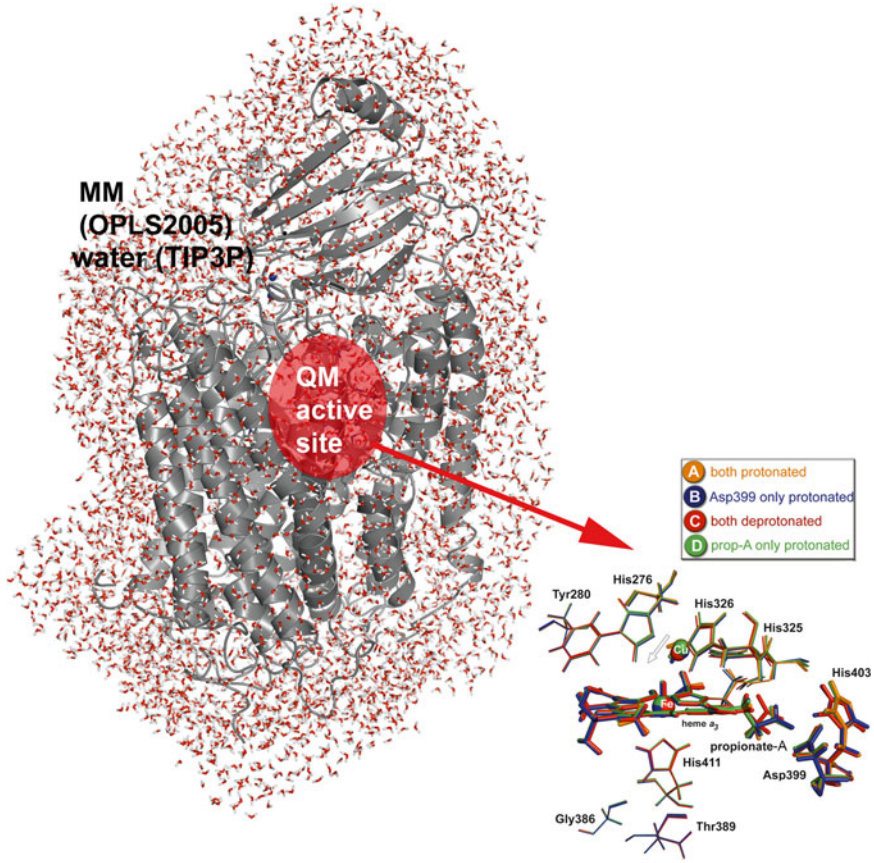

Fig. 10.3. QM/MM model used for the highly elaborate QM/MM calculations, including the whole protein and the water solvent. The active site is represented in QM (DFT) level of theory, while the rest of the protein, as well as the solvent are represented by the OPLS2005/TIP3P Force Fields, respectively. The active site, that is probed at the B3LYP/tzvp* (DFT) level of theory at different protonation states of the Asp399/propionate-A pair, is enlarged on the *bottom right* side of the figure. Cu is optimized at a closer distance to the heme a_3 iron, in the case where the negative charges increase on the Asp399/propionate-A pair.

Waters are possible sites for the accommodation of a proton in the form of transient hydronium (H_3O^+) species, acting as proton carriers. Interestingly, a single water molecule is highly conserved in the crystal structures of bacterial and mammalian CcOs, between the heme a_3 propionates. If such a hydronium molecule interacts with the protein matrix in the area of the heme a_3 propionates, its proton is transferred to the heme a_3 ring A propionate in our QM/MM simulations. This implicates a propionate-D/Arg → prop-A/D399 proton transfer via the conserved water molecule in the cases where a single proton is shared between prop-A and Asp399 (Daskalakis et al. 2011). Figure 10.4 illustrates a schematic mechanism of action involving the early stages of dioxygen activation by CcO. In this model the His403 residue plays the role of a valve, controlling the flow of protons in the region. By substantially changing the pKa values of the prop-A or Asp399, a proton is trapped or released by prop-A. In the closed conformation (strong hydrogen bonding between prop-A and Asp399), the proton is trapped on the prop-A site (Daskalakis et al. 2011). Starting from a structure where a single proton is shared between the latter prop-A/D399 pair (in the oxy intermediate, and the closed His403 conformation), the proton resides 'locked' on the prop-A side. Active site oxidation will trigger

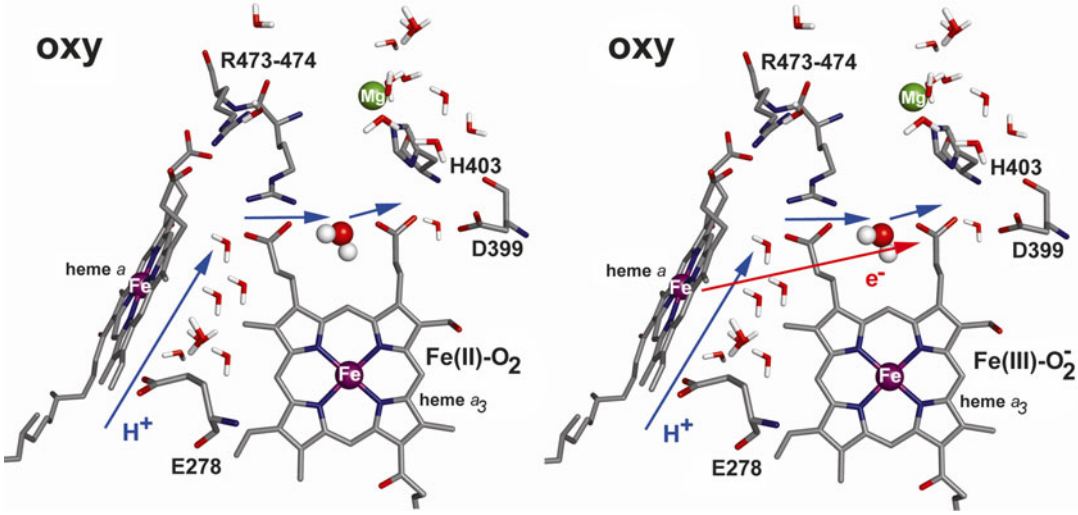

Fig. 10.4. Early stages of CcO dioxygen reaction. The intermediate's oxy are depicted with *arrows* to point the proton (*blue*) and electron (*red*) movement in critical sites around the active site.

the release of that proton as it becomes loosely bound (between prop-A/Asp399) in the rest of the oxidation states and the His403 closed conformation. A water molecule in the area could easily abstract that labile proton. Deprotonation of the prop-A/Asp399 pair increases the presence of negative charges in the area, reallocating Cu_B closer to heme a_3 iron, accommodating also a half spin in prop-A. The heme a_3 Fe(II) is oxidized to Fe(III) upon protonation of the prop-A/Asp399 pair via the D-pathway (Daskalakis et al. 2011). Electron transfer should occur from heme *a*, concurrently to the previous proton transfer, so that the half spin population on prop-A is quenched. This should eventually trigger the further oxidation of the active site to the peroxy and ferryl intermediates. Protonation should change the His403 conformation as discussed previously, thereby trapping the proton on the Asp399 site (His403 open conformation). Another release of a proton to the heme a_3 propionates area via the D-pathway is able to neutralize the prop-A/Asp399 charges and as a consequence His403 residue changes conformation with the protons to become loosely attached to the pair (His403 closed conformation). A water molecule that is leaving the active site can be a possible proton carrier, as well as a trigger for the neutralization of the prop-A/Asp399 pair and the His403 conformational change. In each case, a loosely bound carboxylic proton residing on prop-A/Asp399 is released to the water pool via the Mg that is coordinated to His403 (Schmidt et al. 2003). From the water pool the proton reaches to the solvent immediately, or after His403 changes conformation from open to closed.

B. The Ferryl and Hydroxyl Intermediates

A distal hydrogen bond is the cause of a 20 cm^{-1} shift in (Fe–O) for the hydroxyl intermediate (Fig. 10.2, models 7–8). This distal effect appears significantly enhanced, having twice the amplitude of the proximal effect (Fig. 10.2, models 9–10), partly justifying the proposal of an hydrogen bond in distal region being the cause of the two experimentally observed ν(Fe–O) modes at 450 and 475 cm^{-1} (Han et al. 1989, 2000) for the hydroxyl intermediate.

It is worth noting that the same distal interaction on the ferryl species was calculated to be only 6 cm^{-1} (riBLYP/TZVP level of theory) (Fig. 10.2, models 3–4). The proximal effect on bimetallic (Fe/Cu_B) ferryl complexes accounts for a shift of up to 20 cm^{-1} at the same level of theory (riBLYP/TZVP) and under the same hydrogen bonding network

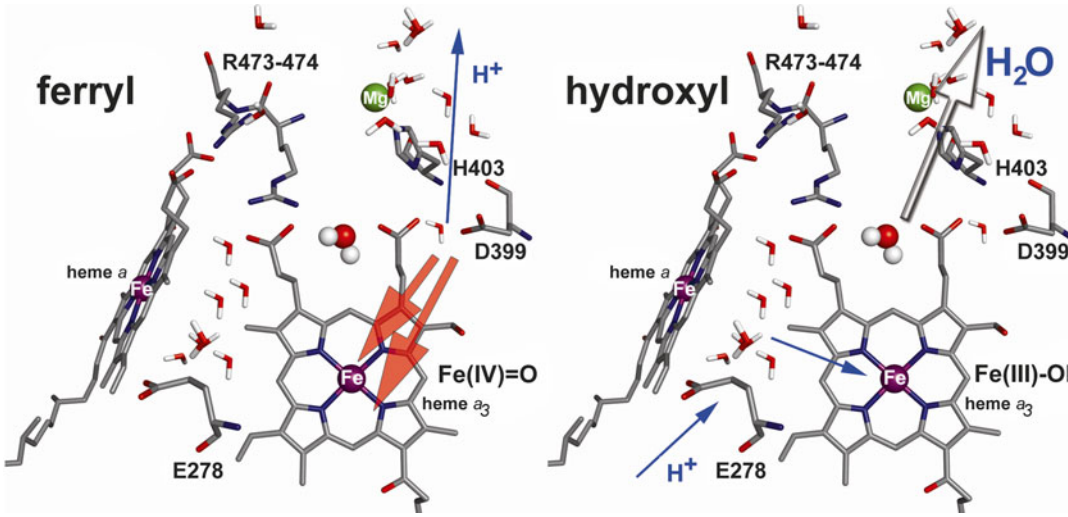

Fig. 10.5. Late stages of CcO dioxygen reaction. The intermediates ferryl and hydroxyl are depicted with *arrows* indicating the proton (*blue*) movement in critical sites around the active site. *Red arrows* are designed to show the effect of the propionate-A site on ferryl heme a_3 Fe=O bond and proximal area characteristics. The *arrow* outlined in *black* depicts the product water movement out of the active site towards the *water pool*.

models (Fig. 10.2, models 1–2) (Pinakoulaki et al. 2013). This pronounced distal effect of the hydroxyl species, is in fact consistent with the advancing of the catalytic cycle. The protonation at the distal site is the key step for the CcO cycle to proceed further, leading to the formation of water molecules at the active site. The presence of H^+ in the distal area should thus immediately affect the hydroxyl Fe(III)–OH moiety and easily induce the transition towards the next step of the catalytic cycle. On the other hand, the presence of H^+ in the distal site at the ferryl intermediate stage does not influence the chemistry of that intermediate. It is proposed that the protonation(s) near the active site (at the heme a_3 propionates area, Fig. 10.3) are communicated to the proximal His (Daskalakis et al. 2008).

Figure 10.5 depicts a schematic view of the last stages of dioxygen activation cycle in CcO. Different protonation states of the prop-A/Asp399 pair control the intensities of the ν(Fe–O) bands (Daskalakis et al. 2008). His403 and Asp399 are connected to Gly386/Thr389 by a short chain of amino acids. Thus, protonation/deprotonation events in the prop-A/Asp399 pair, as well as the His403 conformational changes are communicated via these connecting amino acids to the proximal site of His411. Changes in the hydrogen bonding strengths in the proximal region (Fig. 10.2, models 1–2) are able to control the His411 basicity and thus the ν(Fe–O) modes via resonances (Daskalakis et al. 2010). Glu278 resides at the entrance of the D-pathway. It has been proposed that water molecules are present in the hydrophobic cavity near Glu278, connecting it to the heme a_3 propionate-D and Cu_B (Puustinen et al. 1997; Riistama et al. 1997; Zheng et al. 2003; Olkhova et al. 2004).

In this model, Glu278 has the role of a proton shuttle and/or a valve, mediating the flow of protons towards Cu_B/Fe_{a3} and the propionate-D/Arg salt bridge (Olkhova et al. 2004; Xu and Voth 2005). The propionate-D/Arg salt bridge has been proposed to be in a redox-dependent thermal equilibrium, acting as a gate for a proton or a protonated water molecule (Wikström et al. 2005). As discussed in a previous study (Daskalakis et al. 2011) the Cu_B position is extremely sensitive to the protonation states of the heme a_3 propionates. This thermal equilibrium and proton transient gate should alter the Fe_{a3}–Cu_B distance, which in turn may trigger

vibrational resonances in the His–Fe^{IV}=O ferryl moiety of the active site that are detectable as different bands in resonance Raman spectra (Daskalakis et al. 2010).

IV. Conclusions

We propose the presence of three important aspects in the O_2 reduction cycle in the heme a_3 Fe/Cu_B binuclear center of CcO: (1) The effect from the hydrogen bonding networks proximally to heme a_3 is significantly enhanced only at the ferryl oxidation state. (2) The distal to heme a_3 effect is calculated to be important at the hydroxyl oxidation level. (3) The presence of charges in the vicinity of the active site is crucial to the action mechanism of CcO dioxygen reaction, as it controls the Cu_B position, the His403 conformation (aa_3 from *P. denitrificans* numbering) and consequently the release of protons.

In this chapter we link water and proton motion to spectroscopic characteristics of the active site of CcO. A concerted proton (water mediated) and electron motion has been identified in the case of the oxy intermediate. In hydroxyl and oxy species, the proximal region or the axial His basicity induces extremely weakened changes for the Fe–O/O–O bonds and the respective spectroscopic characteristics. We propose that water and proton motion affect the intensities of the ν(Fe–O)/δ(His–Fe=O) vibrational frequencies and alters the His403 conformation to enable the release of waters/protons out of the heme a_3/Cu_B active site.

Acknowledgments

All calculations have been performed either at the Institute of Electronic Structure and Laser of the Foundation for Research and Technology – Hellas (IESL-FORTH), the Barcelona Supercomputing Center (BSC) at the Life Sciences Department, at the Supercomputing Center in Okazaki National Research Institutes and the European GRID infrastructure (EGEE).

References

Babcock GT, Wikström M (1992) Oxygen activation and the conservation of energy in cell respiration. Nature 356:301–309

Bassan A, Blomberg MRA, Borowski T, Siegbahn PEM (2006) Theoretical studies of enzyme mechanisms involving high-valent iron intermediates. J Inorg Biochem 100:727–743

Belevich I, Verkhovsky MI (2008) Molecular mechanism of proton translocation by cytochrome *c* oxidase. Antiox Redox Signal 10:1–30

Bellevich I, Verkhovsky MI, Wikström M (2006) Proton-coupled electron transfer drives the proton pump of cytochrome c oxidase. Nature 440:829–832

Billingsley FP, Bloor JE (1971) Limited Expansion of Diatomic Overlap (LEDO): a near-accurate approximate *ab initio* LCAO MO method. I. Theory and preliminary investigations. J Chem Phys 55:5178–5190

Blomberg MRA, Siegbahn PEM, Babcock GT, Wikström M (2000a) O-O bond splitting mechanism in cytochrome *c* oxidase. J Inorg Biochem 80:261–269

Blomberg MRA, Siegbahn PEM, Babcock GT, Wikström M (2000b) Modeling cytochrome oxidase – a quantum chemical study of the O-O bond cleavage mechanism. J Am Chem Soc 122:12848–12858

Blomberg MRA, Siegbahn PEM, Babcock GT (2003) Metal-bridging mechanism for O-O bond cleavage in cytochrome C oxidase. Inorg Chem 42:5231–5243

Crane BR, Siegel LM, Getzoff ED (1997) Structures of the siroheme- and Fe4S4-containing active center of sulfite reductase in different states of oxidation: heme activation via reduction-gated exogenous ligand exchange. Biochemistry 36:12101–12119

Daskalakis V, Farantos SC, Varotsis C (2008) Assigning vibrational spectra of ferryl-oxo ontermediates of cytochrome c oxidase by periodic orbits and molecular dynamics. J Am Chem Soc 130:12385–12393

Daskalakis V, Farantos SC, Guallar V, Varotsis C (2010) Vibrational resonances and Cu_B displacement controlled by proton motion in cytochrome c oxidase. J Phys Chem B 114:1136–1143

Daskalakis V, Farantos SC, Guallar V, Varotsis C (2011) Regulation of electron and proton transfer by the protein matrix of cytochrome c oxidase. J Phys Chem B 115:3648–3655

Decatur SM, Belcher KL, Rickert PK, Franzen S, Boxer SG (1999) Hydrogen bonding modulates binding of exogenous ligands in a myoglobin proximal cavity mutant. Biochemistry 38:11086–11092

Eichkorn K, Treutler O, Öhm H, Häser M, Ahlrichs R (1995) Auxiliary basis-sets to approximate coulomb potentials. Chem Phys Lett 240:283–289

Ferguson-Miller S, Babcock GT (1996) Heme/copper terminal oxidases. Chem Rev 96:2889–2908

Gennis RB (1998) Multiple proton-conducting pathways in cytochrome oxidase and a proposed role for the active-site tyrosine. Biochim Biophys Acta 1365:241–248

Goodin DB, McRee DE (1993) The Asp-His-iron triad of cytochrome c peroxidase controls the reduction potential electronic structure, and coupling of the tryptophan free radical to the heme. Biochemistry 32:3313–3324

Han S, Ching YC, Rousseau DL (1989) Evidence for a hydroxide intermediate in cytochrome c oxidase. J Biol Chem 264:6604–6607

Han S, Takahashi S, Rousseau DL (2000) Time-dependence of the catalytic intermediates in cytochrome c oxidase. J Biol Chem 275:1910–1919

Hunsicker-Wang LM, Pacoma RL, Chen Y, Fee JA, Stout CD (2005) A novel cryoprotection scheme for enhancing the diffraction of crystals of recombinant cytochrome ba3 oxidase from *Thermus thermophiles*. Acta Crystallogr Sect D 61:340–343

Iwata S, Ostermeier C, Ludwig B, Michel H (1995) Structure at 2.8 Å resolution of cytochrome c oxidase from *Paracoccus denitrificans*. Nature 376: 660–669

Koepke J, Olkhova E, Angerer H, Müller H, Peng G, Michel H (2009) High resolution crystal structure of *Paracoccus denitrificans* cytochrome c oxidase: new insights into the active site and the proton transfer pathways. Biochim Biophys Acta 1787:635–645

Kozlowski PM, Kuta J, Ohta T, Kitagawa T (2006) Resonance Raman enhancement of Fe–IV=O stretch in high-valent iron porphyrins: an insight from TD-DFT calculations. J Inorg Biochem 100: 744–750

Michel H (1998a) The mechanism of proton pumping by cytochrome c oxidase. Proc Natl Acad Sci USA 95:12819–12824

Michel H (1998b) Cytochrome c oxidase: catalytic cycle and mechanisms of proton pumping – a discussion. Biochemistry 38:15129–15140

Michel H, Behr J, Harrenga A, Kannt A (1998) Cytochrome c oxidase: structure and spectroscopy. Ann Rev Biophys Biom Struct 27:329–356

Ogura T, Hirota S, Proshlyakov DA, Shinzawa-Itoh K, Yoshikawa S, Kitagawa T (1996) Time-resolved resonance Raman rvidence for tight coupling between electron transfer and proton pumping of cytochrome c oxidase upon the change from the Fe^{V} oxidation level to the Fe^{IV} oxidation level. J Am Chem Soc 118:5443–5449

Olkhova E, Hutter C, Lill MA, Helms V, Michel H (2004) Dynamic water networks in cytochrome *c* oxidase from *Paracoccus denitrificans* investigated by molecular dynamics simulations. Biophys J 86:1873–1889

Ostermeier C, Harrenga A, Ermler U, Michel H (1997) Structure at 2.7 Å resolution of the *Paracoccus denitrificans* two-subunit cytochrome c oxidase complexed with an antibody FV fragment. Proc Natl Acad Sci USA 94:10547–10553

Pinakoulaki E, Daskalakis V, Ohta T, Richter O-MH, Budiman K, Kitagawa T, Ludwig B, Varotsis C (2013) The structure of two ferryl-oxo intermediates at the same oxidation level in the heme-copper binuclear center of cytochrome c oxidase: the protein effect. J Biol Chem 288:20261–20266

Puustinen A, Bailey JA, Dyer RB, Mecklenburg SL, Wikström M, Woodruff WH (1997) Fourier transform infrared evidence for connectivity between Cu_B and glutamic acid 286 in cytochrome bo_3 from *Escherichia coli*. Biochemistry 36: 13195–13200

Rauhamäki V, Baumann M, Soliymani R, Puustinen A, Wikström M (2006) Identification of a histidine-tyrosine cross-link in the active site of the *cbb*3-type cytochrome *c* oxidase from *Rhodobacter sphaeroides*. Proc Natl Acad Sci USA 103: 16135–16140

Riistama S, Hummer G, Puustinen A, Dyer RB, Woodruff WH, Wikström M (1997) Bound water in the proton translocation mechanism of the haem-copper oxidases. FEBS Lett 414:275–280

Schmidt B, McCracken J, Ferguson-Miller S (2003) A discrete water exit pathway in the membrane protein cytochrome *c* oxidase. Proc Natl Acad Sci USA 100:15539–15542

Schrodinger Suite of Programs (2010) http://www.schrodinger.com

Soulimane T, Buse G, Bourenkov GP, Bartunik HD, Huber R, Than ME (2000) Structure and mechanism of the aberrant ba3-cytochrome c oxidase from *Thermus thermophilus*. EMBO J 19:1766–1776

Tsukihara T, Aoyama H, Yamashita E, Tomizaki T, Yamaguchi H, Shinzawa-Itoh K, Nakashima R, Yaono R, Yoshikawa S (1995) Structure of metal sites of oxidized bovine heart cytochrome c oxidase at 2.8 Å resolution. Science 269:1069–1074

Turbomole V5–8–0 24 Nov. 2005, University of Karlsruhe

Varotsis C, Babcock GT (1990) Appearance of the $\nu(Fe^{IV}=O)$ vibration from a ferryl-oxo intermediate in the cytochrome oxidase/dioxygen reaction. Biochemistry 29:7357–7362

Vogel KM, Spiro TG, Shelver D, Thorsteinsson MV, Roberts GP (1999) Resonance Raman evidence for a novel charge relay activation mechanism of the CO-dependent heme protein transcription factor CooA. Biochemistry 38:2679–2687

Wikström M (1981) Energy-dependent reversal of the cytochrome oxidase reaction. Proc Natl Acad Sci USA 78:4051–4054

Wikström M (1989) Identification of the electron transfers in cytochrome oxidase that are coupled to proton-pumping. Nature 338:776–778

Wikström M, Ribacka C, Molin M, Laakkonen L, Verkhovsky M, Puustinen A (2005) Gating of proton and water transfer in the respiratory enzyme cytochrome *c* oxidase. Proc Natl Acad Sci USA 102:10478–10481

Xu J, Voth GA (2005) Computer simulation of explicit proton translocation in cytochrome c oxidase. Proc Natl Acad Sci USA 102:6795–6800

Yoshikawa S, Shinzawa-Itoh K, Tsukihara T (1998) Crystal structure of bovine heart cytochrome c oxidase at 2.8 A resolution. J Bioenerg Biomembr 30:7–14

Zheng X, Medvedev DM, Swanson J, Stuchebrukhov AA (2003) Computer simulation of water in cytochrome c oxidase. Biochim Biophys Acta 1557:99–107